NUMERICAL AND EXPERIMENTAL ANALYSIS OF FIN AND TUBE HEAT EXCHANGER

Vladimir Glažar, Bernard Franković, Paolo Blecich
Faculty of Engineering, University of Rijeka, Vukovarska 58, HR-51000 Rijeka,
Tel.: + 385 51 651 536, Fax: + 385 51 675 801,
vladimir.glazar@riteh.hr

Abstract: *In this paper numerical and experimental analysis of compact heat exchanger has been done. A fin and tube heat exchanger composed of four rows of circular tubes has been installed in an open circuit wind tunnel. Air and water were used as working fluids. Same geometry and parameter setup has been analyzed using commercial fluid flow and a heat transfer solver Fluent. Air/water side model has been used because it gives more accurate results than simpler model that includes only air side flow. Comparison between numerical model and experimental results has been accomplished with respect of air and water temperature. It has been shown that numerical model results coincide well with the experimental data, with deviations within an acceptable range. Therefore, used air/water side model can be used for further investigation of more efficient compact heat exchanger geometry.*

Key words: compact heat exchanger, fin and tube, numerical, experimental, air/water model

1. INTRODUCTION

Regarding on construction type, heat exchangers can be divided on tubular, plate-type, regenerative and heat exchangers with extended surfaces [1]. Heat exchangers with extended surfaces are made of elements that are connected to primary surface that is in direct contact with both hot and cold fluid. These elements are referred to as fins. Main use of extended surfaces is to increase the heat transfer area. Compact heat exchangers are widely used in many ways in residential, commercial and industrial HVAC systems [2]. Fin-and-tube heat exchangers are representatives of compact heat exchangers with high compactness ratio. In this paper numerical and experimental analysis of such heat exchanger has been performed. This experimental and numerical investigation has been done as preparation for testing of heat exchangers with microchannel coil. Numerical procedure with air/water side model has been used. When dealing with micro scale channels, scaling effects precisely described by Morini [3] and Rosa [4] should not be neglected. Air/water model, proposed by Borrajo-Pelaez [5], allows implementation of some scaling effects (entrance effects, conjugate heat transfer and viscous heating). Detailed mathematical approach and detailed description of experimental apparatus developed on purpose for this investigation can be found in [6] and [7].

2. EXPERIMENTAL PROCEDURE

2.1. Experimental set-up

Figure 1. shows the schematic diagram of the wind tunnel used in this paper. Air and distilled water were used as working fluids. The main components of the system were compact heat

exchanger, water flow loop, air supply, instrumentations and data acquisition systems. The open circuit wind tunnel system was used to suck air from laboratory or from open air over the air handling unit with capability of air preheating. The speed of centrifugal fan could be adjusted by pressure relief damper from approximately 20 to 100% of maximum air flow. The upper part of tunnel was composed of circular ducts with diameter of ϕ600 mm and lower part from rectangular ducts of appropriate size, 550×450 mm. Measuring station with installed test heat exchanger was insulated with 25 mm thick thermoplastic insulation.

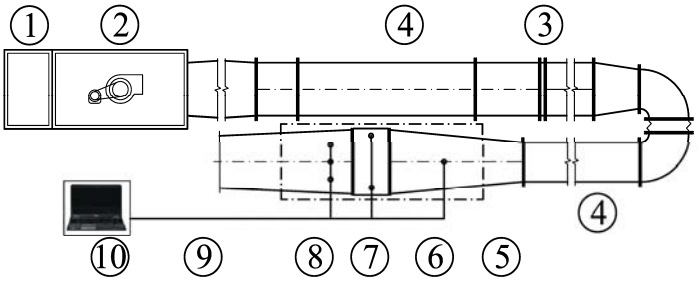

1 air inlet
2 air handling unit
3 orifice
4 air settling ducts
5 measuring station
6 3xPt100 air inlet temperature
7 2xPt100 water in/out temperature
8 9xPt100 air outlet temperature
9 air outlet
10 data acquisition system

Figure 1. Schematic diagram of the wind tunnel test apparatus

The inlet and outlet temperature across air side of the heat exchanger were measured by two platinum resistance thermometer meshes (RTD, Pt100 sensors) shown on Figure 2a. The inlet measuring mesh consisted of three RTD sensors while the outlet mesh consisted of nine RTD sensors. These sensors were connected to data acquisition system in three-wire configuration (Figure 2b). This is relatively simple wiring arrangement that provides accurate readings with reliable auto correction of any problems caused by any effect of the temperature range on the wiring itself. These RTD sensors were pre-calibrated with an accuracy of ±0.15 K. These signals were individually recorded and then averaged.

(a)

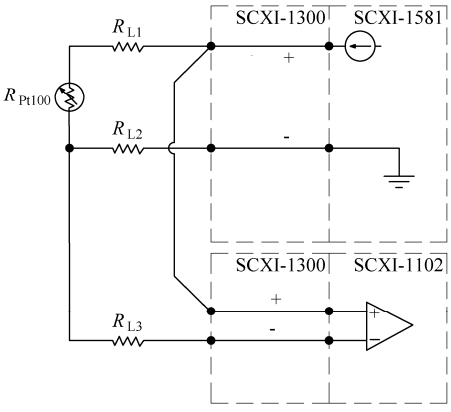

(b)

Figure 2. Platinum resistance thermometer, RTD (a) and schematic diagram of three-wire configuration wiring arrangement (b)

The air flow rate was measured with pipe orifice installed in circular ducts (Figure 3a). A fluid passing through an orifice construction experiences pressure drop. Pressure drop was measured with portable measuring system Testo 350 M/XL which has integrated differential probe. Air flow rate was than calculated from pressure drop achieved on orifice (Figure 3b).

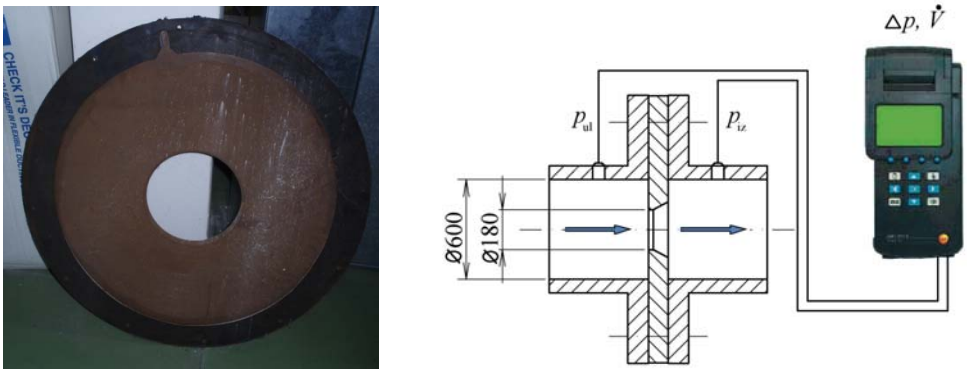

(a) (b)

Figure 3. Pipe orifice (a) and schematic view of portable measuring system *Testo 454* (b)

Water loop was connected to water/water heat pump with capacity of 50 kW. The temperature of the water was measured by the same type of RTD sensors used on air side of wind tunnel. First one was installed on water inlet and other on water outlet. RTD sensors were installed in water stream without direct contact by mean of small tube inserts. Water flow was measured by portable ultrasonic water flow measuring system shown on Figure 4a and b.

(a) (b)

Figure 4. Ultrasonic water flow measuring system *Prosonic flow 92* base unit (a) and clamp-on system connected to pipings (b)

Water loop also consisted of circulating pumps, regulating valves, strainers, expansion tank, pressure gauge and thermometers. Figure 5 shows measuring station of wind tunnel with installed data acquisition system and overall view of used equipment.

(a) (b)

Figure 5. Measuring station of wind tunnel with data acquisition unit (a) and overall view of used equipment (b)

The *National Instruments SCXI* data acquisition, automation and control module system was used (Figure 6a). Connection to personal computer was accomplished by *National Instruments DAQCard* (Figure 6b).

(a) (b)

Figure 6. The National Instruments SCXI data acquisition system (a) and *National Instruments DAQCard* (b)

All virtual instruments were developed in *LabView* which was installed on the computer (Figure 7).

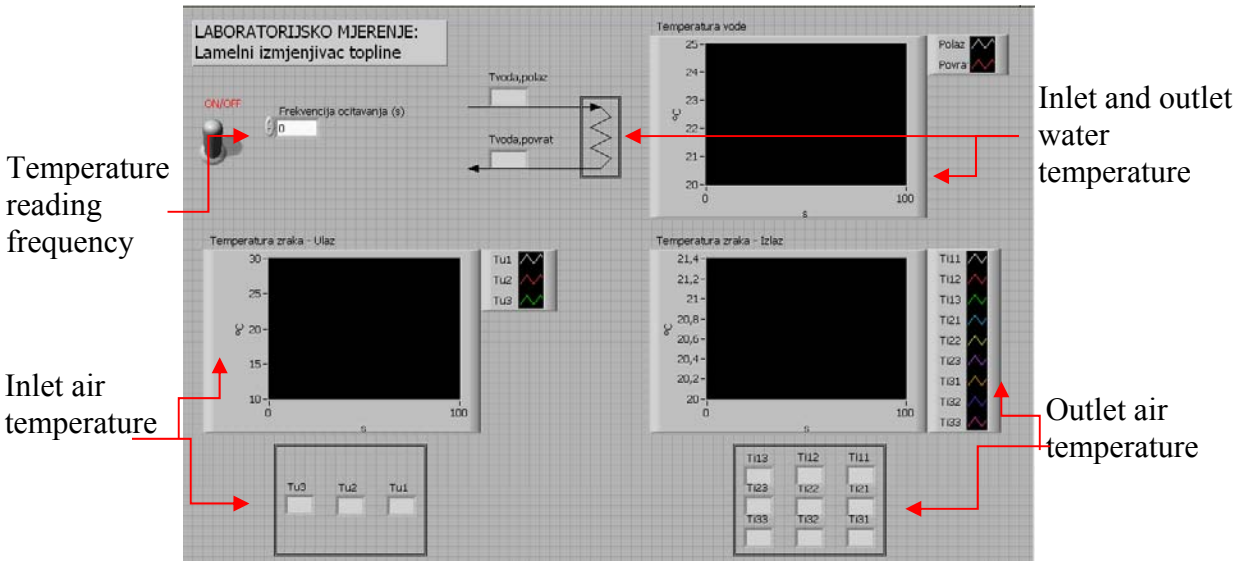

Figure 7. Graphical user interface developed in *LabView*

2.2. Test heat exchanger

Fin-and-tube heat exchanger used in experimental investigation is made of 10 piping loops connected to inlet and outled manifold both positioned on left side of heat exchanger. Heat exchanger has 4 rows configuration. Tubes are connected by 450 wavy fins where fin pitch value (K_l) is 2.2 mm and fin thickness (b_l) is approximately 0.1 mm. Dimension of each tube is ϕ15x1. Examined heat exchanger consists of eight passes on side of the water. First pass is closer to air inlet side. Figure 8 shows schematic diagram of installed heat exchanger.

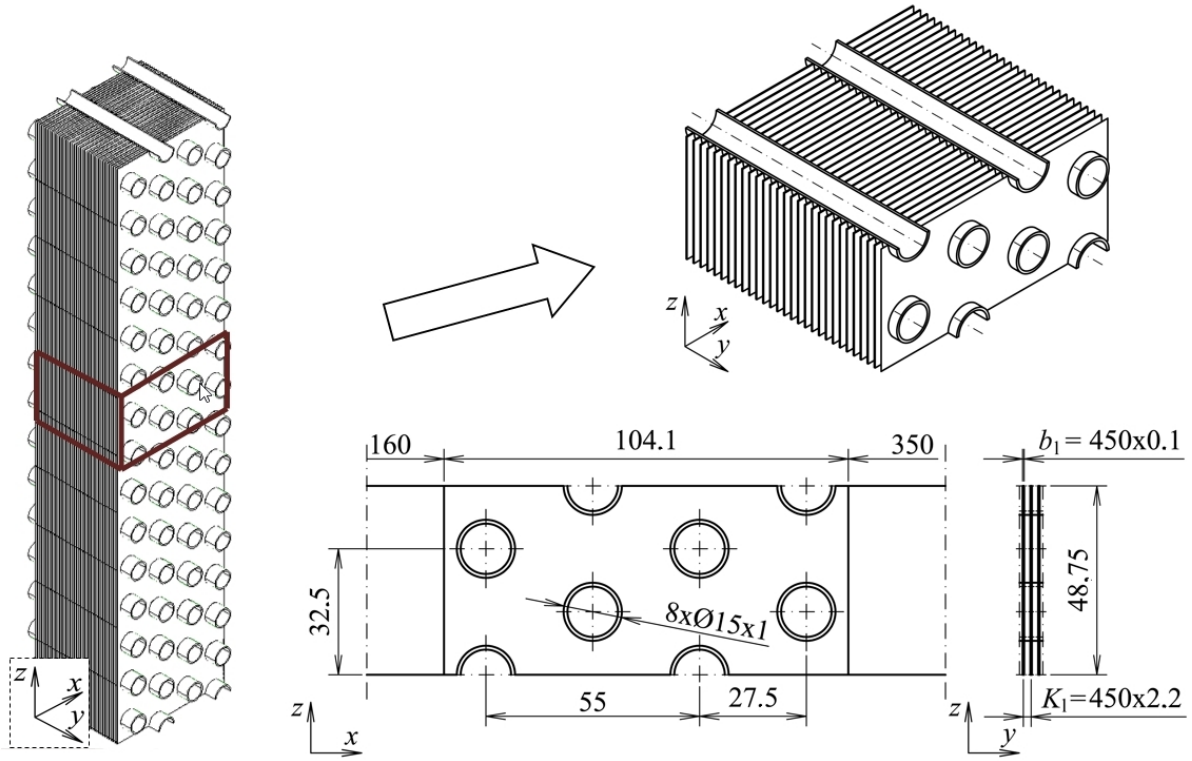

Figure 8. Shematic view of tested fin-and-tube heat exchanger

2.3. Test condition and method

The water tubes were completely insulated with a 10 mm thick layer of thermoplastic insulation. The test was performed in a range of Reynolds number from 50 to 300. Corresponding inlet air velocities were in range from 0.4 to 3 m/s. Reynolds number applied in this calculation is based on hydraulic diameter of fin entrance and maximum air velocity. The water temperature was in range from 305 to 310 K with allowed tolerance of ±1 K per measurement. The choice of water flow rate was based on a principle that a temperature drop on a water side has to be higher than 5 K with constant flow for all measures. Several valid experimental measurements have been taken with different air and water temperatures and flows. Time needed to conclude one measurement was approximately 30 minutes after achievement of appropriate heat balance.

3. NUMERICAL SIMULATION

3.1. Physical and mathematical model

A schematic view of analyzed heat exchanger core is shown on Figure 9. Due to limitations on the computer resources, only portion of the heat exchanger able to describe flows of air and water was taken into account. Two symmetry planes were assumed in the *z*-direction, perpendicular to the fin surface. Both symmetry planes divide two upper tubes in two identical parts.

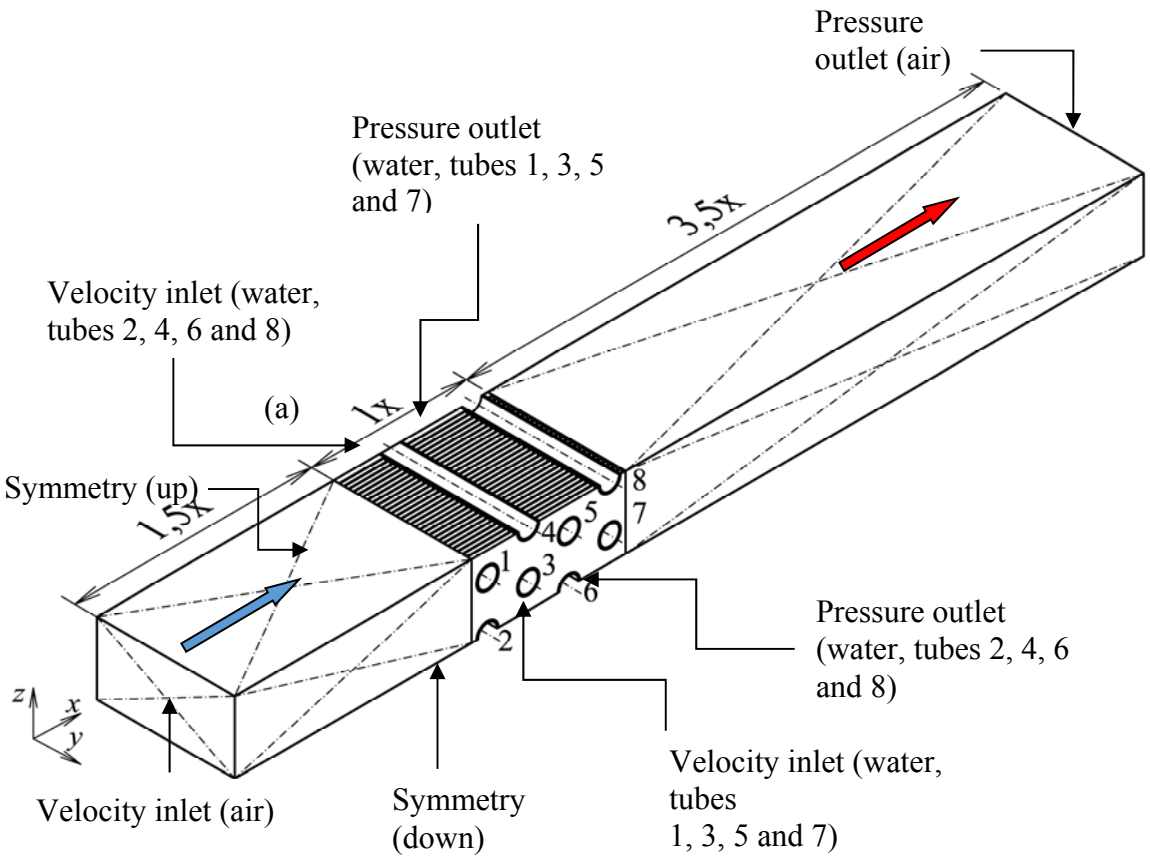

Figure 9. Schematic view of heat exchanger computational domain

The computational domain consists of six volume groups: air upstream and downstream region, water region, internal airspace, fins and eight tubes. Tubes number 1, 3, 5 and 7 were fully modeled, while tubes 2, 4, 6 and 8 were half modeled. The total length of the computational domain has been extended 5 times from actual internal airspace. The upstream region has been extended 1.5 times to ensure inlet uniformity and the downstream region has been extended 3.5 times in order to prevent flow recirculation.

3.2. Governing equations and boundary conditions

The governing equations in the Cartesian coordinate system for forced steady, laminar, incompressible fluid flow and heat transfer in air, water and fin subdomains are:

Air and water subdomain:

Continuity:

$$\operatorname{div}\left(\rho\vec{u}\right)=0 \tag{1}$$

Momentum:

$$\text{x...}\quad \operatorname{div}\left(\rho u\vec{\mathbf{u}}\right)=-\frac{\partial p}{\partial x}+\operatorname{div}\left(\mu\operatorname{grad}u\right) \tag{2}$$

$$\text{y...}\quad \operatorname{div}\left(\rho v\vec{\mathbf{u}}\right)=-\frac{\partial p}{\partial y}+\operatorname{div}\left(\mu\operatorname{grad}v\right) \tag{3}$$

$$\text{z...}\quad \operatorname{div}\left(\rho w\vec{\mathbf{u}}\right)=-\frac{\partial p}{\partial z}+\operatorname{div}\left(\mu\operatorname{grad}w\right) \tag{4}$$

Energy:

$$\operatorname{div}\left(\rho\vec{\mathbf{u}}T_{\mathrm{a}}\right)=\operatorname{div}\left(\frac{k_{\mathrm{a}}}{c_{\mathrm{pa}}}\operatorname{grad}T_{\mathrm{a}}\right) \tag{5}$$

$$\operatorname{div}\left(\rho\vec{\mathbf{u}}T_{\mathrm{w}}\right)=\operatorname{div}\left(\frac{k_{\mathrm{w}}}{c_{\mathrm{pw}}}\operatorname{grad}T_{\mathrm{w}}\right) \tag{6}$$

Fin and tube subdomain:

$$\operatorname{div}\left(\frac{k_{\mathrm{f}}}{c_{\mathrm{pf}}}\operatorname{grad}T_{\mathrm{f}}\right)=0 \tag{7}$$

$$\operatorname{div}\left(\frac{k_{\mathrm{t}}}{c_{\mathrm{pt}}}\operatorname{grad}T_{\mathrm{t}}\right)=0 \tag{8}$$

Boundary conditions are:

At the inlet boundary:

$$u_{\mathrm{a}}=u_{\mathrm{a,in}}=\text{const},\ v=w=0 \tag{9}$$

$$T_{\mathrm{a}}=T_{\mathrm{a,in}}=\text{const} \tag{10}$$

$$v_{\mathrm{w}}=v_{\mathrm{w,in}}=\text{const},\ u=w=0 \tag{11}$$

$$T_{\mathrm{w}}=T_{\mathrm{w,in}}=\text{const} \tag{12}$$

At the outlet boundary:

$$\frac{\partial u}{\partial x}=0,\ \frac{\partial v}{\partial x}=0,\ \frac{\partial w}{\partial x}=0,\ \frac{\partial T_{\mathrm{a}}}{\partial x}=0 \tag{13}$$

$$\frac{\partial u}{\partial y}=0,\ \frac{\partial v}{\partial y}=0,\ \frac{\partial w}{\partial y}=0,\ \frac{\partial T_{\mathrm{w}}}{\partial y}=0 \tag{14}$$

At the front and back boundaries in downstream and upstream region:

$$\frac{\partial u}{\partial y}=\frac{\partial w}{\partial y}=0,\ v=0,\ \frac{\partial T_{\mathrm{a}}}{\partial y}=0 \tag{15}$$

At the upper and lower boundaries in downstream and upstream region:

$$\frac{\partial u}{\partial z}=\frac{\partial w}{\partial z}=0,\ w=0,\ \frac{\partial T_{\mathrm{a}}}{\partial z}=0 \tag{16}$$

At the upper and lower region of air and tube:

$$\frac{\partial u}{\partial z}=\frac{\partial v}{\partial z}=0,\ w=0,\ \frac{\partial T_{\mathrm{a}}}{\partial z}=0 \tag{17}$$

$$\frac{\partial T_{\mathrm{t}}}{\partial z}=0 \tag{18}$$

Air - fin/tube interface:

$$k_{\mathrm{a}}\frac{\partial T_{\mathrm{a}}}{\partial n}=k_{\mathrm{f}}\frac{\partial T_{\mathrm{f}}}{\partial n}=k_{\mathrm{t}}\frac{\partial T_{\mathrm{t}}}{\partial n} \tag{19}$$

3.3. Numerical approach

The governing differential equations were discretized using the finite volume method, fully described by Versteeg and Malalasekera [8], on a hybrid, non-orthogonal grid. The domain has been meshed using GAMBIT. The computational grid is uniform in the *y*-direction. The number of control volumes is close to 55 million divided in 15 computational blocks.

Computational blocks were made due to limitations on the computer resources. Heat transfer and fluid flow simulations were performed using commercial fluid flow and a heat transfer solver FLUENT. All velocity vectors and temperatures between computational blocks were linked with internal scripting language employed in CFD software. Fluid is assumed to be incompressible with constant property values and the flow is assumed to be laminar. The SIMPLE algorithm for pressure-velocity coupling was used to ensure mass conservation and to obtain a pressure field. The convection-diffusion terms have been discretized using the power law scheme.

4. RESULTS AND DISCUSSION

4.1. Matching of computational domain and heat exchanger used in experiment

Figure 10. shows positioning of RTD sensors set for temperature measurement of air leaving heat exchanger relative to computational domain. Temperatures for each point, used in later comparison, have been calculated as average values of three measured temperatures for each RTD sensor column.

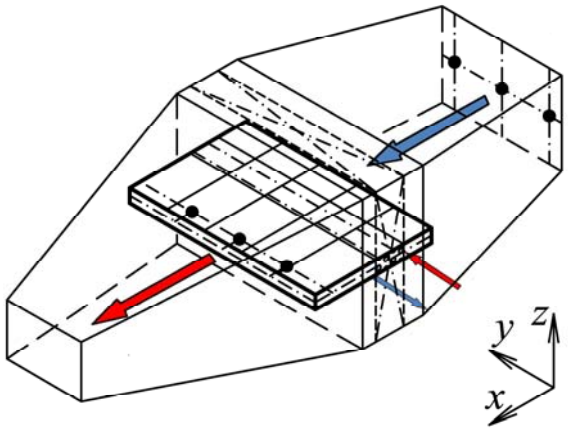

Figure 10. Positioning of RTD sensors in computational domain

4.2. Comparison of numerical and experimental results

Comparison between results acquired with numerical model and experimental results has been accomplished with respect of air and water temperatures. Figure 11. gives comparison of result achieved with both analyses for three different parameter setups described with air inlet temperature ($T_{z,ul}$), air outlet temperature ($T_{z,iz}$), water inlet temperature ($T_{v,ul}$) and water outlet temperature ($T_{v,iz}$).

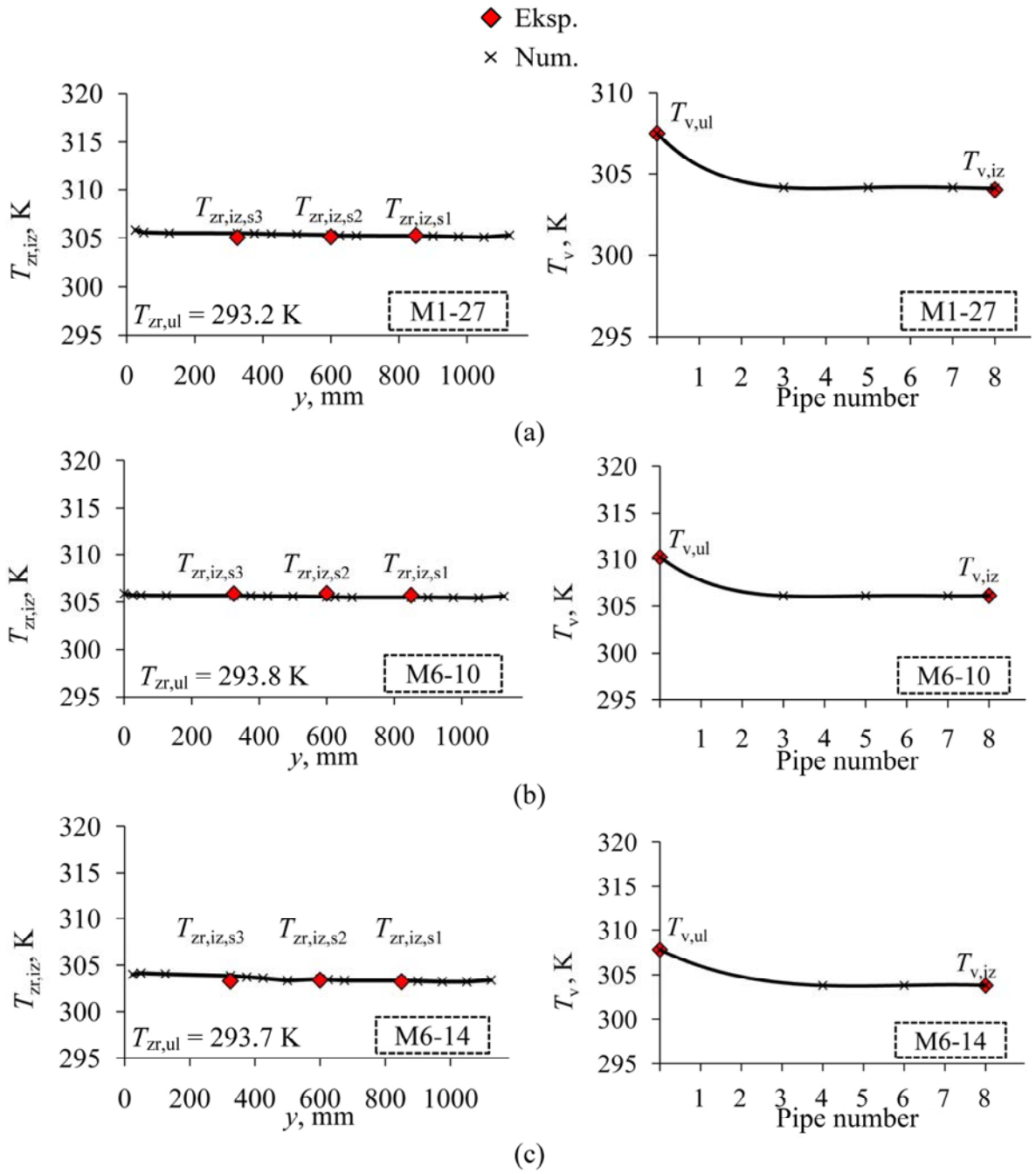

Figure 11. Comparison of acquired results for air inlet velocities 0.8 m/s (a), 1 m/s (b) and 1.2 m/s

5. CONCLUSION

Figure 11. shows that numerical model results coincide well with the experimental data, with deviations within an acceptable range through whole heat exchanger. Air outlet temperature is nearly constant in full range of *y* axes. Reason for that is big number of water passes (eight) that bring stability to heat transfer. Water temperature decreases in first three/four passes, but then stabilizes. This means that heat load of tested heat exchanger was not set at maximum possible.

In this paper comparison has been show only for three parameter setups due to limited paper length. Comparisons for other air and water temperatures and flows have had similar results. Temperature differences were smaller than ±0.5 K for most of the cases what can be taken as

assertion of measurement methodology validity as well as proof of used mathematical model validity. Comparison of two different analyses has been done as a validation of used air/water mathematical model. Therefore, it can be concluded that air/water side model shown in this paper can be used for further investigations of enhanced and improved surface geometries of the fin and tube heat exchangers both on side of water and side of air.

REFERENCES

[1] Shah, R.; Sekulić, D.P.: *Fundamentals of heat exchanger design*, John Wiley & Sons, New York, 2003

[2] Kuppan, T.: *Heat exchanger design handbook,* Marcel Dekker AG, Basel, 2000

[3] Morini, G.L.: *Scaling Effects for Liquid Flows in Microchannels,* Heat Transfer Engineering, 27 (2006), 64-73

[4] Rosa, P.; Karayiannis, T.G.; Collins, M.W.: *Single-phase heat transfer in microchannels: The importance of scaling effects*, Applied Thermal Engineering, 29 (2009), 3447-3468

[5] Borrajo-Pelaez, R.; Ortega-Casanova, J.; Cejudo-Lopez, J.M.: *A three-dimensional numerical study and comparison between the air side model and the air/water side model of a plain fin-and-tube heat exchanger*, Applied Thermal Engineering, 30 (2010), 1608-1615

[6] Glazar, V.: *Compact Heat Exchanger Geometry Optimization*, PhD thesis, Faculty of Engineering University of Rijeka, Croatia (in Croatian), 2011

[7] Glazar, V.; Frankovic, B.; Trp, A.: *Experimental and Numerical Study of the Compact Heat Exchanger with Different Microchannel Shapes*, International Journal of Refrigeration, In Press, Accepted Manuscript, 2014

[8] Versteeg, H.K.; Malalasekera, W.: *An Introduction to Computational Fluid Dynamics, The Finite Volume Method*, Longman Group Ltd, Essex, 1995

NUMERIČKA I EKSPERIMENTALNA ANALIZA CIJEVNOG LAMELNOG IZMJENJIVAČA TOPLINE

Sažetak: *U ovom radu je provedena numerička i eksperimentalna analiza kompaktnog izmjenjivača topline. Cijevni lamelni izmjenjivač topline, sastavljen od okruglih cijevi, je ugrađen u zračni tunel otvorenog tipa. Korišteni radni mediji su zrak i voda. Numeričkim putem je provedena numerička analiza za istu geometriju i postavljene radne uvjete. Numerička analiza je izvršena u komercijalnom paketu za računalnu dinamiku fluida i numeričko modeliranje prijelaza topline Fluent. Korišten je numerički model zrak/voda zato što se pomoću njega postižu precizniji rezultati u odnosu na modele koji uključuju samo stranu zraka. Izvršena je usporedba temperatura zraka i vode dobivenih numeričkim i eksperimentalnim putem. Prikazano je da, uz prihvatljiva odstupanja, rezultati dobiveni numeričkim putem odgovaraju rezultatima dobivenim eksperimentom. Kao zaključak slijedi da se primijenjeni numerički model voda/zrak može koristiti u daljnjem istraživanju s ciljem postizanja geometrije kompaktnih izmjenjivača topline veće učinkovitosti.*

Ključne riječi: kompaktni izmjenjivač topline, cijevni lamelni izmjenjivač topline, numerički, eksperimentalno, model zrak/voda